gallium arsenide substrate. However, a circuit using primarily duroid ($\epsilon_r = 2.2$) as a substrate may use the first low-coupling height ratio with a very thin upper substrate of high dielectric constant inserted above a lower duroid substrate.

Consideration must also be made concerning whether such a mode equalizing structure is physically realizable. Referring to Fig. 2(b), the low-coupling height ratios shown exactly equalize the even- and odd-modes at a given frequency which may not be physically realizable in many circuit designs. However, choosing height combinations as close as possible to these ideal low-coupling height ratios will tend to minimize the overall effects of pulse distortion and coupling in edge-coupled CPW's.

V. Conclusion

A full-wave analysis was used to calculate the effective dielectric constants for even- and odd-modes of edge-coupled, CPW forward directional couplers in multilayer substrate structures using a conductor-backed ground plane. It was found that the phase velocities of both even- and odd-modes can be equalized for specific multilayer substrate height combinations over a wide range of slot geometries, suggesting that a single multilayer substrate configuration may be used to control pulse distortion and coupling for wideband signals. When the lower substrate dielectric constant is much less than the upper substrate dielectric constant, it was found that these low-coupling height combinations can lead to circuit designs using combinations of thick and very thin substrates. Dispersion and coupling of a 10ps Gaussian pulse were presented for uncompensated and compensated configurations. It was shown that a multilayer structure using substrate height combinations that equalize both even- and odd-mode phase velocities can significantly reduce coupling and distortion effects. Design guidelines applicable toward practical MIC and MMIC structures were also presented.

Acknowledgment

The authors would like to thank Drs. J. F. Harvey of the Electronics Division, Army Research Office and J. W. Mink formerly of ARO, for their interest and support of the project.

References

[1] R. L. Veghte and C. A. Balanis, "Dispersion of transient signals in microstrip transmission lines," *IEEE Trans. Microwave Theory Tech.*, vol. MTT-34, pp. 1427–1436, Dec. 1986.

[2] G. Ghione and C. U. Naldi, "Coplanar waveguides for MMIC applications: Effect of upper shielding, conductor backing, finite-extent ground planes, and line-to-line coupling," *IEEE Trans. Microwave Theory Tech.*, vol. MTT-35, pp. 260–267, Mar. 1987.

[3] M. Riaziat, R. Majidi-Ahy, and I. J. Feng, "Propagation modes and dispersion characteristics of coplanar waveguides," *IEEE Trans. Microwave Theory Tech.*, vol. 38, pp. 245–251, Mar. 1990.

[4] K. M. Rahman and C. Nguyen, "On the analysis of single- and multiple-step discontinuities for a shielded three-layer coplanar waveguide," *IEEE Trans. Microwave Theory Tech.*, vol. 41, pp. 1484–1488, Sept. 1993.

[5] M. Riaziat, I. J. Feng, R. Majidi-Ahy, and B. A. Auld, "Single-mode operation of coplanar waveguides," *Electron. Lett.*, vol. 23, no. 24, pp. 1281–1283, Nov. 1987.

[6] J. P. K. Gilb and C. A. Balanis, "Pulse distortion on multilayer coupled microstrip lines," *IEEE Trans. Microwave Theory Tech.*, vol. 37, pp. 1620–1628, Oct. 1989.

[7] Y. Qian, E. Yamashita, and K. Atsuki, "Modal dispersion control and distortion suppression of picosecond pulses in suspended coplanar waveguides," *IEEE Trans. Microwave Theory Tech.*, vol. 40, pp. 1903–1909, Oct. 1992.

[8] G. Hasnain, A. Dienes, and J. R. Whinnery, "Dispersion of picosecond pulses in coplanar transmission lines," *IEEE Trans. Microwave Theory Tech.*, vol. MTT-34, pp. 738–741, June 1986.

[9] P. Singkornrat and J. A. Buck, "Picosecond pulse propagation in coplanar waveguide forward directional couplers," *IEEE Trans. Microwave Theory Tech.*, vol. 39, pp. 1025–1028, June 1991.

[10] H. Baudrand, M. Kaddour, and M. Ahmadpanah, "Bias-variable characteristics of coupled coplanar waveguide on GaAs substrate," *Electron. Lett.*, vol. 23, no. 4, pp. 171–172, 1987.

[11] M. R. Lyons and C. A. Balanis, "Transient coupling reduction in edge-coupled coplanar waveguide forward directional couplers," *IEEE Int. Microwave Symp.*, pp. 1685–1688, May 1994.

[12] T. Itoh and R. Mittra, "Spectral-domain approach for calculating the dispersion characteristics of microstrip lines," *IEEE Trans. Microwave Theory Tech.*, vol. MTT-21, pp. 496–499, July 1973.

[13] T. Uwano and T. Itoh, "Spectral domain approach," in *Numerical Techniques for Microwave and Millimeter-Wave Passive Structures*, T. Itoh, Ed. New York: Wiley, 1989, ch. 5, pp. 334–380.

Computation of Excess Capacitances of Various Strip Discontinuities Using Closed-Form Green's Functions

Kyung S. Oh, Jose E. Schutt-Aine, and Raj Mittra

***Abstract*— An efficient quasi-static method to compute excess (equivalent) capacitances of various strip discontinuities in a multilayered dielectric medium is presented. The excess charge distribution on the surface of a conductor is obtained by solving an integral equation in conjunction with closed-form Green's functions. A complete list of expressions of the closed-form Green's functions for a point charge, a line charge, and a semi-infinite line charge is presented. An open end, a bend, a step junction, and a T junction are considered as numerical examples.**

I. Introduction

Quasi-static analysis is often performed to characterize strip discontinuities when the dimensions of the discontinuities are much smaller than the wavelength. Under the quasi-static analysis, the dominant effect of strip discontinuities is fringing fields due to the physical irregularities of discontinuity geometries. The modeling of these fringing fields in terms of an excess capacitance is discussed in this paper.

Numerous papers have been published to compute excess capacitances of various microstrip discontinuities, and a summary of popular methods can be found in [1]. The most successful approach is one based on the formulation of an integral equation in terms of the excess charge distribution, which was first proposed by Silvester and Benedek [2] and has been applied to analyze various microstrip discontinuities [2]–[5]. The Green's function for a layered medium is employed in this approach. For N dielectric layers, the expression for this Green's function would consist of an $N-1$ nested infinite series [6]; hence, in practice, this form of the Green's function may

Manuscript received February 17, 1995; revised January 17, 1996. This work was supported in part by the Joint Services Electronics Program Grant N00014-96-1-0129.

The authors are with the Department of Electrical and Computer Engineering, University of Illinois at Urbana-Champaign, Urbana, IL 61801-2991 USA.

Publisher Item Identifier S 0018-9480(96)03032-3.

not be applied to a multilayered medium. Recently, Sarkar *et al.* [7] solved discontinuity problems for a multilayered medium using the free-space Green's function, but additional unknown charges (over unknown charges on the surface of a conductor) had to be placed on the dielectric interfaces and the top ground plane to model the polarization charge and the free charge. Although such inclusion of unknowns may be tolerable for two-dimensional (2-D) problems, it is computationally too burdensome for three-dimensional (3-D) problems.

In this paper, the closed-form Green's function discussed in [8] is employed to formulate an integral equation in terms of the excess charge distribution. A complete list of expressions of the closed-form Green's functions for a point charge, a line charge, and a semi-infinite line charge with or without a top ground plane is presented in this paper. The presented method requires neither additional unknowns to model dielectric interfaces and the top ground plane nor evaluations of any infinite series except for cases where the top ground plane is present. When the top ground plane is present, using the closed-form Green's function is still numerically advantageous since the nested infinite series in the expression of the usual Green's function becomes a simple infinite series without nesting.

II. Closed-Form Green's Functions

Closed-form expressions of the electrostatic Green's functions for a point charge, a line charge, and a semi-infinite line charge are derived in this section based on the approach used in [8]. Consider N dielectric layers which are backed by a ground plane as depicted in Fig. 1. The Nth layer is either a half-space or terminated by an optional top ground plane. All dielectric layers and ground planes are assumed to be planar and infinite in the xz-plane. The electrostatic Green's function in the spectral domain is described by the following closed-form formula [8]:

$$\begin{aligned}\tilde{G}(\gamma, y|r_0) &= \frac{1}{2\varepsilon_m\gamma}(K_1^+(\gamma,m,n)e^{\gamma(y+y_0-2d_n)} + K_2^+(\gamma,m,n) \\ &\cdot e^{\gamma(y-y_o+2(d_{m-1}-d_n))} + K_3^+(\gamma,m,n)e^{\gamma(-y+y_o)} \\ &+ K_4^+(\gamma,m,n)e^{\gamma(-y-y_o+2d_{m-1})}) \qquad y \geq y_o \end{aligned} \tag{1a}$$

$$\begin{aligned}\tilde{G}(\gamma, y|r_o) &= \frac{1}{2\varepsilon m\gamma}(K_1^-(\gamma,m,n)e^{\gamma(y+y_o-2d_m)} + K_2^-(\gamma,m,n) \\ &\cdot e^{\gamma(y-y_o)} + K_3^-(\gamma,m,n)e^{\gamma(-y+y_o+2(d_{n-1}-d_m))} \\ &+ K_4^-(\gamma,m,n)e^{\gamma(-y-y_o+2d_{n-1})}) \qquad y \leq y_o \end{aligned} \tag{1b}$$

where $\tilde{G}$ is the spectral-domain Green's function, and r and r_o are the observation and source points located in the nth and mth layers, respectively. The superscripts $+$ and $-$ are used to denote the cases for $y \geq y_o$ and $y \leq y_o$. The expressions for the four coefficient functions $K_i^{\pm}$ can be found in [8]. A closed-form expression of the Green's function in the space domain is obtained by approximating these four coefficient functions $K_i^{\pm}$ using exponential functions. It is important to mention that although $K_i^{\pm}$ is dependent on m and n, it is not a function of y and y_o; hence, the approximation can be performed without any prior knowledge of the junction geometry. The following two subsections detail the derivation of the closed-form Green's functions due to a point charge, a line charge, and a semi-infinite line charge with or without the top ground plane.

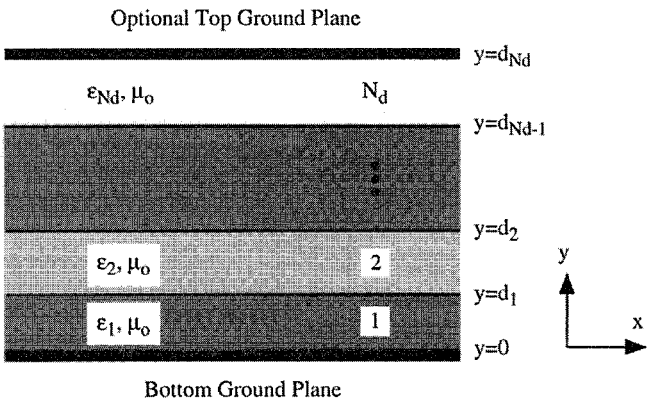

Fig. 1. Cross-sectional view of a multilayered dielectric medium.

A. Closed-Form Green's Functions for Geometries Without the Top Ground Plane

When there is no top ground plane, the four coefficient functions $K_i^{\pm}$ in (1a) or (1b) are nonoscillatory and smooth functions of γ; hence, each coefficient function can be accurately approximated with real-valued exponential functions as follows [8]:

$$K_i^{\pm}(m,n,\gamma) = \sum_{j=1}^{N_{m,n,i}^{\pm}} C_{m,n,i}^{\pm,j} e^{\alpha_{m,n,i}^{\pm,j}\gamma}, \qquad i = 1,2,3,4 \tag{2}$$

where $N_{m,n,i}^{\pm}$ denotes the number of exponential functions used in the approximation of $K_i^{\pm}$, which typically ranges from 5 to 10. The exponential functions used in the spectral-domain approximation can be physically interpreted as weighted images in the space domain [8]. Compared to the exact Green's function in the space domain, which consists of an infinite number of images, the expression for the closed-form Green's function consists of only a finite number of weighted images.

Once the exponential approximation is performed in the spectral domain, the closed-form Green's functions for 2-D and 3-D can be obtained in the space domain by using the inverse Fourier transformation formulas (14a) and (14b) in [8], and the resulting expressions are given by

$$G^{2D}(\rho|\rho_o) = -\frac{1}{2\pi\varepsilon_m}\sum_{i=1}^{4} f_i^{2D,\pi}(\rho|\rho_o) \tag{3a}$$

$$G^{3D}(r|r_o) = \frac{1}{4\pi\varepsilon_m}\sum_{i=1}^{4} f_i^{3D,\pm}(r|r_o). \tag{3b}$$

For $i = 1$ and $y \leq y_o$, the expressions of $f_i^{2D,\pm}$ and $f_i^{3D,\pm}$ are given by (4a) and (4b) as shown at the bottom of the page.

$$f_1^{2D,+}(\rho|\rho_o) = \sum_{j=1}^{N_{m,n,1}^{+}} C_{m,n,1}^{+,j} \cdot \ln\left(\sqrt{(x-x_o)^2 + (y+y_o-2d_n+a_{m,n,1}^{+,j})^2}\right) \tag{4a}$$

$$f_1^{3D,+}(r|r_o) = \sum_{j=1}^{N_{m,n,1}^{+}} \frac{C_{m,n,1}^{+,j}}{\sqrt{(x-x_o)^2 - (y+y_o-2d_n+a_{m,n,1}^{+,j})^2 + (z-z_o)^2}} \tag{4b}$$

Similar expressions can be obtained for $f_i^{2D\pm}$ and $f_i^{3D,\pm}$ for other values of i.

To derive the Green's function for a semi-infinite uniform line charge, the auxiliary Green's function for a line charge with polarity reversal is employed [2]. Consider a uniform line charge, which starts from $z = \xi$ and is infinitely extended in the positive z-direction; then the Green's function for a semi-infinite line charge G^{semi} can be expressed as

$$G^{\text{semi}}(r|r_o,\xi) = \tfrac{1}{2}[G^{2D}(\rho|\rho_o) + G^p(r|r_o,\xi)] \tag{5}$$

where G^{semi} is the Green's function for a line charge with an abrupt polarity reversed from minus to plus at $z = \xi$. The expression for G^p is obtained by integrating the potential due to a point charge [2]

$$\begin{aligned} G^p(r|r_o,\xi) &= -\int_{-\infty}^{\xi} G^{3D}(r|r_o) + \int_{\xi}^{\infty} G^{3D}(r|r_o) \\ &= \frac{1}{4\pi\varepsilon_m}\sum_{i=1}^{4} f_i^{p,\pm}(r|r_o,\xi) \end{aligned} \tag{6}$$

Again, for $i = 1$ and $y \le y_o$, $f_i^{p,\pm}$ is given by (7) as shown at the bottom of the page.

B. Closed-Form Green's Functions for Geometries with the Top Ground Plane

When the top ground plane is present, all of the four coefficient functions $K_i^{\pm}$ are still nonoscillatory but contain a pole at $\gamma = 0$; as a consequence, $K_i^{\pm}$ can no longer be accurately approximated with exponential functions [8]. To overcome this difficulty, let us rewrite $\tilde{G}$ in the following manner:

$$\tilde{G}(\gamma,y|r_o) = R_{m,n}\tilde{G}^h(\gamma,y|r_o) + \tilde{G}'(\gamma,y|r_o) \tag{8}$$

where $\tilde{G}^h$ is the spectral-domain Green's function for a homogeneous medium, i.e., all dielectric layers are replaced by the source layer. $R_{m,n}$ is a constant which is determined such that $\tilde{G}^h$ contains a pole at $\gamma = 0$ and $\tilde{G}'$ is a well-behaved function without any poles. $R_{m,n}$ can be obtained either numerically or analytically by taking limits of $\tilde{G}$ and $\tilde{G}^h$ as $\gamma \to 0$. Now the technique used in the previous section can be applied to obtain the closed-form expression for $\tilde{G}'$ in the space domain, and the space-domain expressions of $\tilde{G}$ are obtained once the corresponding expressions of $\tilde{G}^h$ are determined.

Expressions of $\tilde{G}^h$ in the space domain can be easily obtained using the image theory approach and are given by

$$G^{2D,h}(\rho|\rho_o) = -\frac{1}{2\pi}\sum_{k=-\infty}^{\infty} \ln\left(\frac{\sqrt{(x-x_o)^2+(y-y_o-2kh)^2}}{\sqrt{(x-x_o)^2+(y+y_o-2kh)^2}}\right) \tag{9a}$$

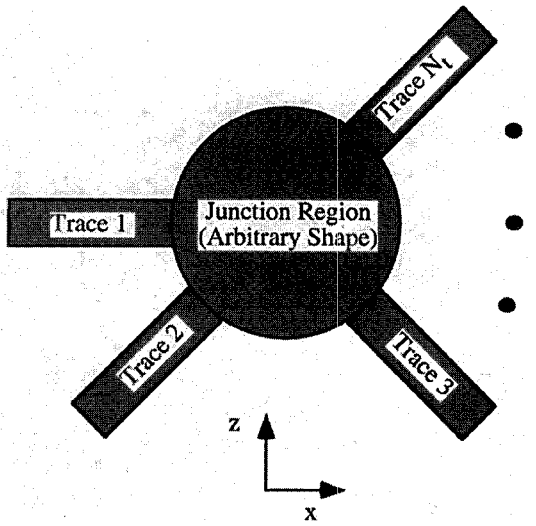

Fig. 2. General geometry of a strip discontinuity.

$$\begin{aligned} G^{3D,h}(r|r_o) &= \frac{1}{4\pi}\sum_{k=-\infty}^{\infty} \\ &\cdot\left(\frac{1}{\sqrt{(x-x_o)^2+(y-y_o-2kh)^2+(z-z_o)^2}}\right. \\ &\left. -\frac{1}{\sqrt{(x-x_o)^2+(y+y_o-2kh)^2+(z-z_o)^2}}\right) \end{aligned} \tag{9b}$$

and (9c) as shown at the bottom of the page.

Unfortunately, all expressions are written in terms of infinite series. Although $G^{2D,h}$ can be alternatively expressed using a closed-form formula [8], such closed-form formulas cannot be been found for $G^{3D,h}$ and $G^{p,h}$. Since the closed-form formula for $G^{2D,h}$ requires numerical integration when the moment matrix is computed, we will simply use (10a) to evaluate $G^{2D,h}$. Therefore, an infinite-series expression, in general, cannot be avoided for G^{2D}, G^{3D}, and G^p when the top ground plane is present. However, the expressions for G^{2D}, G^{3D}, and G^p given in this paper are still numerically more efficient than the ones obtained from the conventional image method since a nested infinite series of the conventional method is reduced to a simple infinite series without nesting as shown in the above equations.[1] For this reason we shall still refer to G^{2D}, G^{3D}, and G^p given by (9), (10a), (10b), and (10c) as closed-form Green's functions.

[1] Alternatively, infinite series can be avoided by modeling the top ground plane as an additional conductor and using the Green's functions in the previous section.

$$f_1^{p,+}(r|r_o,\xi) = \sum_{j=1}^{N_{m,n,1}^{+}} C_{m,n,1}^{+,j}\cdot\ln\left(\frac{\sqrt{(x-x_o)^2+(y+y_o-2d_n+a_{m,n,1}^{+,j})^2+(z-\xi)^2}+(z-\xi)}{\sqrt{(x-x_o)^2+(y+y_o-2d_n+a_{m,n,1}^{+,j})^2+(z-\xi)^2}-(z-\xi)}\right) \tag{7}$$

$$\begin{aligned} G^{p,h}(r|r_o,\xi) = \frac{1}{4\pi}\sum_{k=-\infty}^{\infty} \ln\left(\frac{\sqrt{(x-x_o)^2+(y-y_o-2kh)^2+(z-\xi)^2}+(z-\xi)}{\sqrt{(x-x_o)^2+(y-y_o-2kh)^2+(z-\xi)^2}-(z-\xi)}\right. \\ \left.\cdot\frac{\sqrt{(x-x_o)^2+(y+y_o-2kh)^2+(z-\xi)^2}-(z-\xi)}{\sqrt{(x-x_o)^2+(y+y_o-2kh)^2+(z-\xi)^2}+(z-\xi)}\right). \end{aligned} \tag{9c}$$

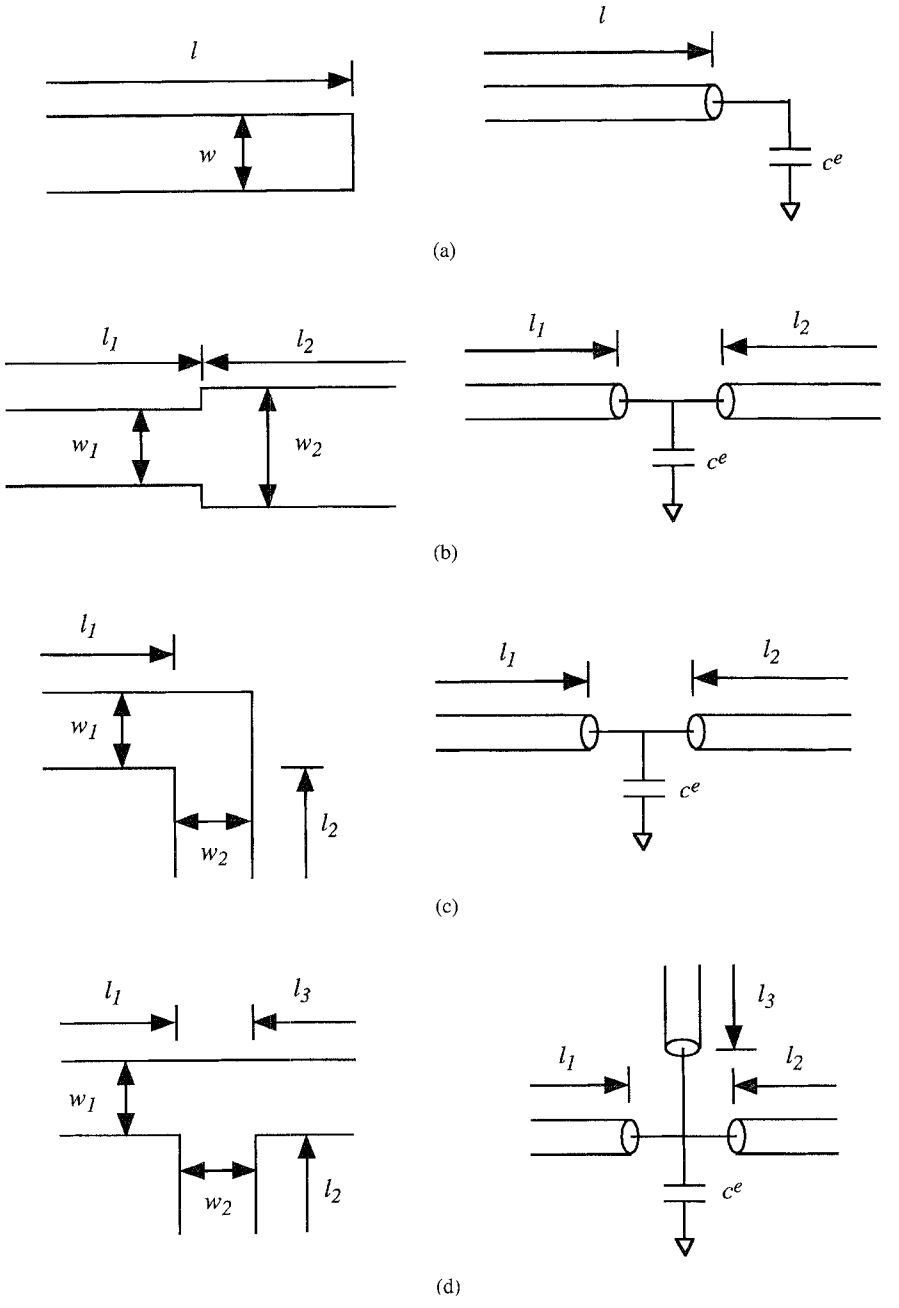

Fig. 3. Discontinuities and their equivalent circuit representations. (a) An open end. (b) A step junction. (c) A bend. (d) A T junction

III. Formulation of an Integral Equation

In this section, an integral equation is formulated in terms of the excess charge distribution using the closed-form Green's functions derived in the previous section. Fig. 2 shows the planar view of the general geometry of a discontinuity, which consists of traces and a junction region. This general geometry represents most of the common strip discontinuities, e.g., an open-end, a nonothogonal bend, and various junctions. Although the present approach can handle conductors with finite thicknesses, the conductor thicknesses are assumed to be infinitely thin in this paper. The discontinuity structure is embedded in a layered dielectric medium, which is shown in Fig. 1.

The integral equation relating the electrostatic potential ϕ and the charge density q on the surface of a conductor is given by

$$\phi(r) = \int_{\Omega} G^{3D}(r|r')q(r')\,dr' = \langle G^{3D}, q\rangle \tag{10}$$

where Ω are the surfaces of a conductor: traces and a junction region. To simplify the notation the integration is symbolically written as $\langle\cdot,\cdot\rangle$. Now let us rewrite the charge density q in the following manner:

$$q(r) = \begin{cases} q_J(r), & \text{if } r \text{ is on the junction region} \\ q_T^i(r), & \text{if } r \text{ is on the } i\text{th trace} \end{cases} \tag{11}$$

Then, (10) becomes

$$\phi(r) = \langle G^{3D}, q\rangle = \langle G^{3D}, q_J\rangle + \sum_{i=1}^{N_t} \langle G^{3D}, q_T^i\rangle. \tag{12}$$

Decomposing the charge densities q_T^i into the uniform charge density $q_T^{\text{unif},i}$ and the excess charge density $q_T^{\text{excess},i}$ for each trace

$$q_T^i(r) = q_T^{\text{unif},i}(r) + q_T^{\text{excess},i}(r). \tag{13}$$

TABLE I
THE NUMERICAL RESULTS (UNITS ARE IN FEMTOFARAD)

	Medium 1		Medium 2	Medium 3
	Computation	Others	Computation	Computation
Open End	17.33	17.0 [1]	23.52	19.62
Step Junction	1.120	1.05 [1], 0.74 [7]	1.352	0.609
Bend	6.210	6.75 [1], 5.8 [7]	7.006	9.184
T Junction	1.385	1.9 [7]	-4.917	-0.818

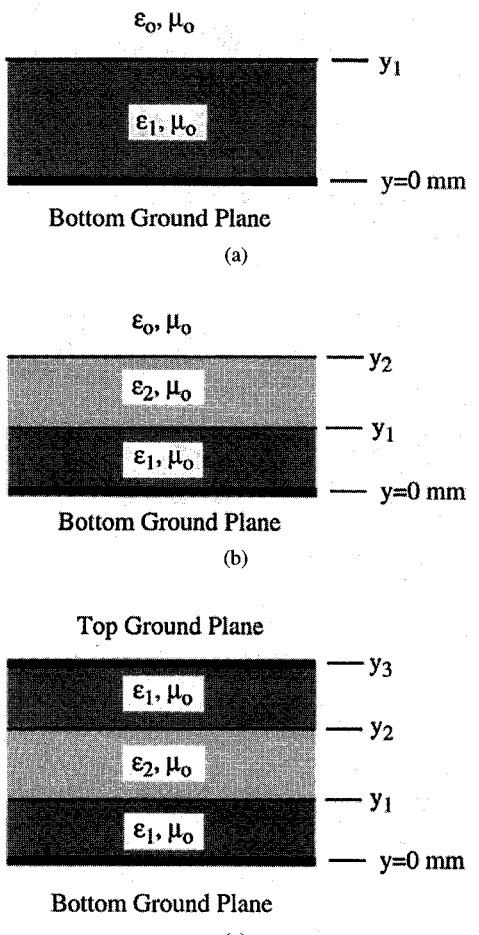

Fig. 4. Three media considered for numerical examples. (a) Medium 1. (b) Medium 2. (c) Medium 3.

Here, the uniform charge density $q_T^{\mathrm{unif},i}$ is obtained by solving a 2-D problem, in which it is assumed that only the ith trace is present in the medium and that the ith trace is infinitely long in both directions. A detailed discussion for solving 2-D problems is given in [8]. The uniform charge density $q_T^{\mathrm{unif},i}$ exists only on the ith trace, which is a semi-infinite line; hence, G^{semi} should be used to compute the potential due to $q_T^{\mathrm{unif},i}$. Using (13), (12) can be written as follows:

$$\phi(r) - \sum_{i=1}^{N_t} \langle G^{\mathrm{semi}}, q_T^{\mathrm{unif},i} \rangle = \langle G^{\mathrm{3D}}, q_J \rangle + \sum_{i=1}^{N_t} \langle G^{\mathrm{3D}}, q_T^{\mathrm{excess},i} \rangle \quad (14)$$

The integral equation (14) can now be solved by using the method of moments. The collocation method is used in this paper. The closed-form formula for the integration involving G^{3D} is given discussed in [8], whereas the integration involving G^{semi} can be analytically integrated using the following formula:

$$\begin{aligned}
&\int_{l_1}^{l_2} \ln\left[\frac{\sqrt{a^2+b^2+l^2}+a}{\sqrt{a^2+b^2+l^2}-a}\right] dl \\
&\quad = 2|b|\left[\tan^{-1}\left(\frac{al_1}{|b|\sqrt{a^2+b^2+l_1^2}}\right)\right. \\
&\qquad \left. - \tan^{-1}\left(\frac{al_2}{|b|\sqrt{a^2+b^2+l_2^2}}\right)\right] \\
&\qquad + 2a\ln\left(\frac{l_2+\sqrt{a^2+b^2+l_2^2}}{l_1+\sqrt{a^2+b^2+l_1^2}}\right) \\
&\qquad + l_2\ln\left(\frac{\sqrt{a^2+b^2+l_2^2}+a}{\sqrt{a^2+b^2+l_2^2}-a}\right) \\
&\qquad - l_1\ln\left(\frac{\sqrt{a^2+b^2+l_1^2}+a}{\sqrt{a^2+b^2+l_1^2}-a}\right).
\end{aligned} \quad (15)$$

Now once (15) is solved, the excess (equivalent) capacitance c^e can be obtained by

$$c^e = \left[Q_J + \sum_{i=1}^{N_T} Q_T^{\mathrm{excess},i}\right] \Big/ \phi_o \quad (16)$$

where Q_J is the total charge on the junction region, and $Q_T^{\mathrm{excess},i}$ is the total excess charge on the ith trace. Throughout the formulation, we have assumed that the junction region exists between traces. The formulation for cases without the junction region, such as an open end and step junctions, can be easily obtained simply by removing terms corresponding to q_J.

IV. NUMERICAL EXAMPLES

Excess capacitances for four common strip discontinuities, an open end, a step junction, a bend, and a T junction, are computed. The geometries of discontinuities with their corresponding equivalent circuits are shown in Fig. 3. The following parameters are used: 1) an open end: $w = 0.5$ mm, 2) a step junction: $w_1 = 0.1$ mm and $w_2 = 0.2$ mm, 3) a right-angle bend: $w_1 = w_2 = 0.15$ mm, and 4) a T junction: $w_1 = w_2 = w_3 = 0.15$ mm. Three different types

of media are considered for each discontinuity with the following parameters (see Fig. 4): 1) an open end: $\varepsilon_1 = 4.2, \varepsilon_2 = 2.5, y_1 = 1.0$ mm, $y_2 = 1.5$ mm, and $y_3 = 2.0$ mm, 2) a step junction: $\varepsilon_1 = 6.0, \varepsilon_2 = 4.2, y_1 = 0.1$ mm, $y_2 = 0.2$ mm, and $y_3 = 0.3$ mm, 3) a bend: $\varepsilon_1 = 2.5, \varepsilon_2 = 4.2, y_1 = 0.15$ mm, $y_2 = 0.3$ mm, and $y_3 = 0.5$ mm, 4) a T junction: $\varepsilon_1 = 2.5, \varepsilon_2 = 4.2, y_1 = 0.15$ mm, $y_2 = 0.3$ mm, and $y_3 = 0.5$ mm. All discontinuities are assumed to be embedded at $y = y_1$. To place 3-D unknowns for the excess charge distribution, the length of each trace is truncated at $l = 8w$. The total numbers of unknowns per each trace were 50 for a 2-D problem and 160 for a 3-D problem, whereas 100 unknowns were used for the junction region. The maximum number of exponentials used to approximate each coefficient function $K_i^{\pm}$ was 5.

The computed results are shown in Table I with the comparison data for a microstrip case [Fig. 4(a)]. A good agreement was found overall as shown in the table. It is interesting to note that for some cases the value of an excess capacitance turns out to be negative. Although a physical capacitance must be positive, an excess (equivalent) capacitance is hypothetical and can be negative.

V. Conclusion and Future Work

An efficient method to compute excess capacitances of strip discontinuities was discussed in this paper. Complete expressions of closed-form Green's functions for a point charge, a line charge, and a semi-infinite line charge have been derived. Unlike other approaches, only a single integral equation is employed in this paper to handle various strip discontinuities instead of formulating an integral equation for each discontinuity type.

References

[1] K. C. Gupta, R. Garg, and I. J. Bahl, *Microstrip Lines and Slotlines*. Norwood, MA Artech House, 1979.

[2] P. Silvester and P. B. Benedek, "Equivalent capacitances of microstrip open circuits," *IEEE Trans Microwave Theory Tech.*, vol. 20, pp. 511–516, Aug. 1972

[3] P. B. Benedek and P. Silvester, "Equivalent capacitances for microstrip gaps and steps," *IEEE Trans. Microwave Theory Tech.*, vol 20, pp 729–733, Nov. 1972.

[4] P. Silvester and P. B Benedek, "Microstrip discontinuity capacitances for right-angle bends, T junctions, and crossings," *IEEE Trans Microwave Theory Tech.*, vol. 21, pp. 341–346, May 1973.

[5] ——, "Correction to 'Microstrip discontinuity capacitances for right-angle bends, T junctions, and crossings,'" *IEEE Trans. Microwave Theory Tech.*, vol. 23, p. 456, May, 1975.

[6] C. Wei, R. F. Harrington, J. R. Mautz, and T. K. Sarkar, "Multiconductor transmission lines in multilayered dielectric media," *IEEE Trans. Microwave Theory Tech.*, vol. 32, pp. 439–450, Apr. 1984.

[7] T. K. Sarkar, Z. A. Maricevic, J. B. Zhang, and A. R. Djordjevic, "Evaluation of excess inductance and capacitance of microstrip junctions," *IEEE Trans. Microwave Theory Tech.*, vol. 42, pp. 1095–1097, June 1994.

[8] K. S. Oh, D. B. Kuznetsov, and J. E. Schutt-Aine, "Capacitance computations in a multilayered dielectric medium using closed-form spatial Green's functions," *IEEE Trans. Microwave Theory Tech.*, vol. 42, pp. 1443–1453, Aug 1994.